c-di-GMP is required for swarming motility in *E. coli*

YuneSahng Hwang, Marta Perez, Rebecca Holzel and Rasika M. Harshey*

Department of Molecular Biosciences and

LaMontagne Center for Infectious Diseases,

The University of Texas at Austin,

Austin, Texas, 78712, USA

* Corresponding author: rasika@austin.utexas.edu

Abstract

Many bacteria use flagella to swim individually through bulk liquid, or swarm collectively over a semi-solid surface. In *E. coli*, elevated levels of c-di-GMP inhibit both chemotaxis and swimming speed via the effector protein YcgR, which when complexed with c-di-GMP, skews the motor bias to CCW and slows the motor. We show in this study that contrary to its effect on swimming, a certain threshold level of c-di-GMP is required for swarming. Gene expression profiles during the time course of swarming first indicated that the patterns of c-di-GMP-related enzymes were altered, and of these, we found that *dgcM* and *dgcO* both played a role in swarming - the former was required for optimal swarming, while the latter was more critical. We report that DgcO promotes production of colanic acid - one of the three major exopolymers in *E. coli* – and show for the first time that colanic acid has surfactant properties that likely aid in swarming. Our findings not only uncover a new role for c-di-GMP in enhancing surface motility but also provide an explanation for why *E. coli* requires additional components such as glucose for effective swarming.

Importance

It is well-established that in bacteria, c-di-GMP inhibits flagella-driven motility at various points in the pathway – gene expression, flagella assembly, flagella rotation. Concomitantly, elevated c-di-GMP levels induce the expression and synthesis of a variety of exopolysaccharides that enmesh the bacteria in a biofilm, thereby also interfering with flagella function. This study reports the surprising finding that in *E. coli*, the exopolysaccharide colanic acid is required to enable surface navigation and that the diguanylate cyclase DgcO is employed for this purpose. For surface navigation, there appears to be a sweet spot where c-di-GMP levels are just right to produce polysaccharides that can serve as surfactants and wetting agents rather than promote formation of biofilms.

Introduction

c-di-GMP signaling offers bacteria lifestyle choices, the most prevalent being a choice between moving freely or settling in a biofilm [1-3]. *E. coli* has 12 diguanylate cyclases (DGCs) that synthesize c-di-GMP and 13 phosphodiesterases (PDEs) that degrade it [4]. In free-swimming or planktonic *E. coli*, DgcN, DgcO, DgcQ and DgcE are reported to be some of the most active DGCs, and PdeH the most active PDE [5-7]. Elevated c-di-GMP levels resulting from the inactivation of PdeH inhibit swimming motility but have only a moderate effect on swarming [8]. The inhibitory effect of c-di-GMP on swimming is well-studied and is orchestrated via the effector protein YcgR. Briefly, YcgR::c-di-GMP binds to both the flagellar switch complex and the stators to first alter the bias to CCW, thus interfering with chemotaxis, and then slow motor speed to eventually stop rotation [5, 8-13]. High levels of c-di-GMP promote biofilm formation [1, 3, 14]. *E. coli* biofilms consist of various extracellular polymers and polysaccharides [15], including cellulose, curli fimbriae, and poly-β-1,6-N-acetyl-d-glucosamine (PGA) [2].

The present study is largely concerned with flagella-driven swarming motility, where bacteria move collectively on a surface. It is now well-appreciated that swarming presents unique challenges not encountered while swimming [16, 17]. These include limited water availability on the surface necessary for flagella to work, and daunting physical forces that bacteria must overcome such as surface tension, friction, and viscosity. Bacteria have evolved various strategies to overcome these challenges, such as secreting wetting agents (generally polysaccharides) to draw water to the surface, surfactants to reduce surface tension, altering cell shape to improve side-by-side alignment and to overcome viscosity during collective motion, and increasing flagella numbers or recruiting special stator-associated proteins that enhance motor power [17-19]. Swarming is typically observed in the laboratory on media solidified with agar, whose consistency can range from semi-solid to solid depending on the agar concentration (0.5%-0.7% or 1-2% w/v), presenting differing levels of navigational

challenge. Bacteria that only swarm on the lower range of agar concentration have been classified as 'temperate', and those that swarm on the higher range as 'robust' swarmers [17]. *E. coli* and *Salmonella* swarmers belong to the former category, while *Proteus mirabilis* and *Vibrio parahaemolyticus* fall under the robust category; the latter set of bacteria increase flagella production to enhance motor power. Some temperate swarmers like *Serratia marcescens* and *Bacillus subtilis* secrete copious amounts of surfactants and/or increase flagella numbers [19].

E. coli and *Salmonella* neither increase flagella numbers nor are reported to secrete specific surfactants [20-23]. These bacteria require nutrient-rich media for swarming, with *E. coli* being particularly fastidious, needing in addition 0.5% glucose and a specific type of agar (Eiken agar) that is more 'wettable' [23, 24]. Two studies suggested that lipopolysaccharide (LPS) might serve to attract water in these bacteria [25, 26], and two others implicated an additional role for flagella rotation in enabling a wet surface [27, 28]. One of these studies identified non-swarming mutants in the LPS biosynthetic pathway of *Salmonella* and suggested that the hydrophilic nature of LPS may serve as a wetting agent [25}, while the other detected high osmotic pressure at the leading edge of an *E. coli* swarm using fluorescent liposomes, and suggested that a secreted high molecular weight substance (perhaps LPS) extracts water from the underlying agar to enable motility [26]. We note that the term ‘wetting agent’ and ‘surfactant’ have been used interchangeably in the literature; here we will use it to mean ‘ability to attract water’. Microarray data showed that LPS synthesis was upregulated specifically in *Salmonella* swarms [29]. Non-swarming mutants of *Salmonella* also mapped to the colanic acid (CA) biosynthesis pathway [25]. CA is a polyanionic heteropolysaccharide composed of repeating hexo-saccharides, that is required for the normal *E. coli* biofilm architecture [15], and could also serve as a potential secreted wetting agent [25].

The present study was initiated to understand the significance of the differential expression of several DGCs and PDEs observed in RNAseq data collected over a time course of *E. coli* swarming. Deletion analysis of the upregulated genes indicated that only absence of

DgcM and DgcO had a negative effect on swarming, the absence of DgcO being critical. DgcM has been reported to regulate the production of curli fibers through the *csgABC* operon [30-32]; curli fibers are crucial for cell-to-cell and cell-to-surface interactions, as well as for the maintenance and stability of biofilms [33, 34]. DgcO, formerly identified as DosC, is a well-characterized DGC, recognized for its ability to bind oxygen via its heme domain [35], and to affect PGA (poly-beta-1,6-GlcNAc) synthesis [36]. We have investigated the role of DgcO, the more critical of the two DGCs, in some detail and found that the swarming defect is caused primarily by a lack of CA production; expression of some CA biosynthesis genes was upregulated during swarming. We find that along with its expected wetting properties, CA has hitherto unknown surfactant properties that likely assist swarming.

Results and Discussion

DgcO plays a critical role in swarming

Deletion of the most active PDE *pdeH* in *E. coli* suppresses swimming but has little to no effect on swarming (Fig. S1A) [8]. Using a riboswitch-based c-di-GMP sensor that enables the measurement of intracellular c-di-GMP levels [37], we compared the relative levels of c-di-GMP in both planktonic (refered to henceforth as 'swim') and swarm cells (Table 1; see Methods). Deletion of *pdeH* produced a much larger increase of c-di-GMP levels in swim compared to swarm cells (Fig. S1B), explaining the differential effect of Δ*pdeH* on motility under the two conditions. This result motivated us to examine RNAseq data generated in our lab as part of a different project (M. Perez, unpublished data) for expression patterns of DGCs and PDEs during the time course (2-20 h) of *E. coli* swarming. Compared to swim cells, we observed that of the 12 DGCs, the expression of *dgcJ, dgcM, dgcO* was elevated ~3-8 fold during this time course (Fig. 1A). Among the PDEs, *pdeH* was drastically downregulated during swarming, with a reduction of over 100-fold in the measured raw values (Fig. S1C),

explaining why deletion of this PDE has a larger effect on swimming compared to swarming (Fig. S1A-B), while *pdeO* and *pdeR* were significantly upregulated (Fig. S1C). The contribution of the upregulated DGCs and PDEs to both swimming swarming was investigated next by deleting them individually (Fig. 1B, C and Fig. S1D). Deletion of *dgcJ* did not perturb swimming, but showed a slight increase in swarming, consistent with our prior results showing that expression of this DGC has a negative effect only during swarming [38]. Deletion of *dgcM* decreased both swimming and swarming (the latter more significant if the plates were allowed to dry longer prior to inoculation), while deletion of *dgcO* had a consistently worse outcome only for swarming, not for swimming (Fig. 1C). In contrast, deletion of both *pdeO* and *pdeR* had no effect on swarming (Fig. S1D). Surprisingly, when Δ*dgcO* cells were observed under the microscope at 4h, a time point when movement begins in WT, they were seen moving as well as WT (Movies S1 & S2). It appears then that the *dgcO* mutant was motile but unable to advance across the surface.

We conclude that both DgcM and DgcO play a positive role specifically during swarming, with DgcO being the dominant player. Going forward, we focused on the contribution of DgcO.

c-di-GMP is required for swarming

Overexpression of DgcO is known to enhance the production of poly-N-acetyl glucosamine (PGA) via the c-di-GMP signaling pathway; PGA serves as an adhesin for the maintenance of biofilm structural stability in diverse eubacteria [36]. Complementation of Δ*dgcO* with a plasmid encoding *dgcO* driven from pBAD promoter (pDgcO) partially rescued the swarming defect without added arabinose inducer (i.e. leaky expression; Fig. 2A); addition of arabinose inhibited rescue, suggesting that a narrow range of c-di-GMP levels elicited the observed swarming phenotype (see Table 1 for c-di-GMP levels under these conditions). To test

whether the swarming defect of Δ*dgcO* is related solely to alterations in c-di-GMP levels, we introduced a plasmid encoding *dgcN* ($_p$DgcN), one of the more active *E. coli* DGCs, into the mutant strain. Leaky expression was sufficient to rescue swarming, while addition of inducer was inhibitory (Fig. 2A and Table 1). Both sets of results suggest that a certain threshold level of c-di-GMP is required for swarming, beyond which it is inhibitory. Swarming inhibition observed by induction of pDgcN was relieved by deletion of *ycgR*, showing that the inhibition at higher levels of c-di-GMP is due to interference with flagellar motor function as established in studies on swimming (Fig. S2). To confirm the assessment that a threshold level of c-di-GMP is important for swarming using an alternate approach, we reduced c-di-GMP levels in the WT by introducing a plasmid expressing *pdeH* (pPdeH) under the control of an IPTG-inducible promoter. Addition of IPTG with as low a concentration as 10 μM reduced c-di-GMP levels below WT (Table 1) and inhibited swarming (Fig. 2B), but did not affect swimming (Fig. 2C, right). We note that the ability to complement Δ*dgcO* with a heterologous DGC does not rule out a specific function for DgcO, as is the case for some DGCs [39, 40].

Next, we measured intracellular c-di-GMP levels in the different genetic backgrounds described above using the biosensor in cells taken directly from the swarm and swim plates shown in Figure 2A and B (see Table 1). There was a correspondence between the extent of swarming (Fig. 2C, left) and measured cellular c-di-GMP levels (Fig. 2D, left). This correspondence did not hold for swimming.

We conclude that a narrow concentration range of c-di-GMP supports optimal swarming in *E. coli*, with levels below WT or above a certain threshold being inhibitory.

Identifying downstream effectors of c-di-GMP action during swarming

To investigate how c-di-GMP positively regulates swarming motility, we looked for suppressors that would restore swarming in a *ΔdgcO* strain. Among the 10 suppressors

selected for whole-genome sequencing, mutation in *yhbX*, which codes for a putative inner membrane hydrolase with no known function, was identified in 9 out of 10 cases, each time at the same nucleotide (Table 2). The second most common mutation was in *fhuA*, followed by *stfP*. FlhuA is a ferrichrome outer membrane receptor involved in TonB-dependent ferrichrome transport [24], and *stfP* is annotated as a cryptic lambdoid prophage protein. We then separately transduced gene deletions in *yhbX* and *fhuA* from the Keio collection into Δ*dgcO* strain, as well as deleted *stfP* using recombineering. Only Δ*fhuA* successfully rescued swarming (Fig. 3A). The rescue is likely related to the importance of a threshold level of intracellular iron for swarming in *E. coli* [41], as also observed in *S. marcescens* [42]. Suppression of the *ΔdgcO* defect by *ΔflhuA* is likely not directly related to DgcO activity but is an alternate rescue mechanism, as c-di-GMP levels remained the same in *ΔdgcOΔfhuA* strain (Table 1).

Since the Δ*dgcO* strain can begin movement on a swarm plate (Movie S2) but not progress outward, and since the ability of a swarm to progress requires that bacteria produce surfactants and/or wetting agents, we next wondered if the mutant might be defective in the production of polysaccharides, suspected to contribute to wetting the agar. DGCs are known to regulate polysaccharide production crucial for formation and maintenance of biofilms [2, 3, 43, 44]. In *E. coli*, DgcC directly regulates cellulose synthesis, while PGA synthesis is mediated by *dgcO* [36]. In *Salmonella*, AdrA upregulates CA biosynthesis [45]. In *P. aeruginosa*, the DGC SadC interacts with a partner protein WarA to modify the LPS O-antigen [46].

We therefore examined the RNAseq data for changes in all high MW exopolymers – LPS, CA, PGA, cellulose - during the time course of swarming. Of these, several genes in the CA (especially *wcaF* and *wcaJ)* and cellulose biosynthetic pathways were upregulated during swarming (Fig. 3B). However, our WT MG1655 strain has a defect in cellulose production [47], so we focused on examining the contribution of colanic acid to swarming in the Δ*dgcO* strain.

Using qRT-PCR, we confirmed that the expression level of *wcaJ* was significantly lower in the *ΔdgcO* strain compared to the WT (Fig. 3C), suggesting a possible involvement of this DGC in CA synthesis.

Colanic acid is important for swarming

To test whether CA positively regulates swarming, we constructed two mutant strains: *ΔwcaJ* and *ΔwaaF*. *wcaJ* is part of a multi-gene operon that controls CA biosynthesis [48]; deletion of this gene does not affect LPS synthesis. *waaF* belongs to a multi-gene operon controlling LPS biosynthesis [49]; deletion of this gene not only produces a defect in the LPS core, but also overproduces CA, possibly via the RcsCDB system [49]. *ΔwcaJ* showed a severe swarming defect (Fig. 4A). The *ΔwaaF* strain could not be tested for swarming because overproduction of CA inhibits flagella biosynthesis [49]. We therefore extracted CA from the *ΔwaaF* strain (see Methods) and added it to the non-swarming *ΔwcaJ* strain directly on the swarm plate to test if external supplementation would rescue the swarming defect (Fig. 4A). Through trial and error, we identified an amount of the extract that fully complemented the *ΔwcaJ* defect (Fig. 4A, +CA). It's important to note that adding the same volume of water as a control was not effective, nor was a similar extract made from the *ΔwcaJ* strain (Fig. 4A).

To ensure that our CA extracts were not contaminated with LPS [48, 50], we compared these extracts with those of LPS extracted from the WT strain [50] after fractionation on polyacrylamide gels (SDS-PAGE), followed by silver staining, a standard method used to characterize LPS [51]. The series of bands corresponding WT LPS extract, were absent in the CA extracts of the *wcaJ* and *waaF* mutants (Fig. S3). We conclude that CA and not LPS complements the *wcaJ* mutant of *E. coli* for swarming.

To determine if the swarming defect of *ΔdgcO* is due to a lack of CA production, we first measured their levels in this strain (see Methods) (Fig. 4B). The *ΔdgcO* strain showed a

significant decrease in CA production compared to the WT strain, confirming that DgcO plays a role in CA synthesis. Additionally, leaky expression from DgcN was sufficient to rescue CA levels in *ΔdgcO,* showing that c-di-GMP is required for maintaining CA production (Fig.4B). CA extract prepared from the *ΔwaaF* strain rescued swarming in *ΔdgcO*, the swarm diameter showing a positive correlation with the amount of CA added (Fig. 4C). Taken together, the data in Figure 4A-C allow us to conclude that DgcO is important for regulating the production of CA, which is a critical component of surface movement of *E. coli*. We have not investigated the nature of this control.

Addition of glucose rescues *ΔdgcO* swarm defect

The availability of glucose has been reported to stimulate the Rcs regulon [48] , and it is well-established that *E. coli* requires 0.5% glucose for optimal swarming. This dependency was traditionally attributed to the need for maintaining motility, given the energy-intensive nature of the swarming process [52, 53]. However, examination of *E. coli* cells inoculated on swarm plates with either 0% or 0.5% glucose (Movie S3 and S4) revealed that cells were similarly motile on both plates. Considering that addition of CA can rescue *ΔdgcO* cells from the swarm defect (Fig. 4C) and that glucose can enhance CA production, we hypothesized that glucose might play additional roles on to facilitate swarming in *E. coli*. Specifically, we tested whether the addition of glucose could bypass the requirement for c-di-GMP signaling and enable the *ΔdgcO* strain to overcome its swarming defect. We therefore supplemented swarm plates with either 0.2% or 1% glucose (w/v) and assessed the swarm motility of four different *E. coli* strains: WT, *ΔdgcO, ΔwaaF*, and *ΔwcaJ*. The *ΔdgcO* strain demonstrated a full restoration of swarming motility at 1% glucose, suggesting that glucose addition directly upregulated CA production, as previously reported [48], bypassing the need for c-di-GMP signaling in the CA pathway. In contrast, the *ΔwcaJ* strain showed only a slight increase in swarm diameter despite glucose stimulation, likely due to the absence of a key component of the CA pathway

in this mutant (Fig. 4D). These results support our conclusion that CA is important for *E. coli* swarming.

PGA is semi-essential for swarming, cellulose is not

In *E. coli*, both PGA and cellulose are regulated by c-di-GMP signaling [30, 34, 36, 54, 55]. To test the role of PGA in swarming, we constructed two mutant strains, *ΔpgaA* and *ΔpgaB*, that are crucial for PGA production. Neither strain was defective in swimming (Fig. S4A). Under standard conditions for preparing swarm plates, where we dry freshly poured plates for 1 h in a hood under laminar flow, these mutants were not significantly impaired for swarming compared to WT (Fig. S4B, top row). However, when the plates were dried for an extra 30 min (1.5h), a noticeable decrease in swarming was observed in the mutants compared to the WT. In *ΔpgaA*, this defect was overcome upon expressing expressing *pgaA* from a plasmid (pPgaA), suggesting that PGA plays a niche role for *E. coli* motility on drier surfaces.

MG1655, the *E. coli* strain used in our study contains a mutation in the *bcsQ* gene in the cellulose synthesis pathway, that introduces an early stop codon, similar to many strains derived from the K-12 lineage [56]. This mutation results in reduced cellulose production compared to other *E. coli* strains, such as enteroaggregative (EAEC) that are known to form a robust biofilm complex. To assess the role of cellulose in swarming motility, we reversed the premature stop codon by introducing a single mutation in codon 6 (TAG→TTG, A17T) of *bcsQ* to restore cellulose production as previously reported [47]. Indirect measurement of cellulose using crystal violet staining indicated a significant increase in staining (Fig. S4C). However, the reverted strain did no better than the original in swarming, even when plates were dried for an extra 30 minutes (Fig. S4D). From these experiments, we conclude that among the three polymers *E. coli* secretes, CA plays a major role, PGA a secondary role, and cellulose no role in swarming motility. We note that the robust swarmers *P. mirabilis* and *V.*

parahaemolyticus both produce abundant capsular polysaccharides; for *P. mirabilis*, these are required for swarming [57, 58]. Proteins that control capsular polysaccharide synthesis in *V. parahaemolyticus* have GGDEF and EAL signatures.

Colanic acid acts as a surfactant

To investigate how CA assists swarming motility, we had a choice between a wetting or a surfactant function. CA fits the former bill, but we decided to evaluate the latter as well. To do so, we conducted a drop collapse test, a method commonly used to assay surfactants [21], where the curvature angle of the droplet is inversely correlated with its surfactant capacity. CA was extracted from the swarming cells of WT, *ΔwcaJ*, and *ΔwaaF* strains. The extracts were then filtered to remove any remaining bacteria and placed on a clean plastic surface, along with water as control. The curvature angle of the *ΔwcaJ* extract was comparable to that of water, whereas the *ΔwaaF* extract showed a significant decrease (Fig. 5A, B), suggesting that colanic acid indeed has surfactant properties. Next, we compared the curvature angle of these extracts when placed directly on swarm plates (outline marked with red-dotted lines) by capturing a close-up, top-view image of the drop with a Nikon D200 camera (Fig. 5C, left). The angle θ (°) between the drop and the surface was calculated using a spherical cap approximation θ=720·$V\pi$2·a3 (*V*: volume of the drop, a: radius (mm)), as previously described [21] (Fig. 5C, right). Since *E. coli* will swarm on medium set with Eiken agar but not Fisher agar, we first measured how a water drop behaved immediately after being added to the surface of the two kinds of plates. The Fisher agar plate showed a significantly higher contact angle, indicating it is less wettable than Eiken agar plates, as had hypothesized earlier ([23, 59]). The CA extract from Δ*waaF* placed on Eiken agar had the lowest contact angle, demonstrating greater wettability than the water-supplemented plates. This result suggests that the addition of CA effectively lowers surface tension not only on plastic but even on swarm agar plates. In summary, these data confirm that CA functions as a surfactant.

Summary

This study reports the following discoveries related to the role of c-di-GMP during swarming in *E. coli*: 1. DgcO and DgcM are upregulated during swarming. 2. A threshold amount of c-di-GMP is required for swarming. 3. DgcO plays a major role in producing the requisite c-di-GMP levels, while DgcM plays a secondary role. 4. DgcO promotes CA synthesis, which facilitates swarming. 5. CA has surfactant properties that likely aid swarming. 5. PGA, also known to be controlled by DgcO ([36]), plays a secondary role when swarming on drier surfaces. These findings are summarized in Figure 6.

Overall, this study reinforces the notion that secreted polysaccharides play an important role in flagella-driven surface navigation. The new finding is that c-di-GMP is an important player in CA production in *E. coli*. The study also shows that there is a narrow window of c-di-GMP concentrations, and by extrapolation, polysaccharide amounts, within which movement is facilitated. While the role of negatively charged, hydrophilic polysaccharides as wetting agents in attracting water to the surface is recognized from past studies, that they could also serve as surfactants is a new finding. What surface cues lead to upregulation of DgcO, and at what point this DGC feeds into the CA pathway is not addressed in this study. We note that DgcO possesses a heme domain that interacts with oxygen [35, 60], suggesting that oxygen availability in the swarm might modulate its activity. However, mutations in DgcO reported to interfere with heme binding did not produce the Δ*dgcO* swarming phenotype (data not shown). A particularly gratifying aspect of this study is understanding why the *E. coli* strain we employ in our swarming studies needs a special agar and the critical addition of glucose, a feature identified 30 years ago [23]. Glucose stimulates CA synthesis, which acts as a surfactant and likely also as a wetting agent.

Acknowledgments

The c-di-GMP sensor was generously provided by Dr. Tai, Jung-Shen from Dr. Yan's lab, Yale University. We thank Souvik Bhattacharyya for helpful comments during the course of this work, which was supported by NIH grant GM118085.

Methods

Strains, growth conditions, mutagenesis, and plasmid constructions

Strains and plasmids used in this study are listed in **Table S1**. The WT parent strain for *E. coli* was MG1655 for all experiments. All strains were grown in LB broth (10 g/liter tryptone, 5 g/liter yeast extract, 5 g/liter NaCl). When appropriate, the following antibiotics were used: Ampicillin (100 μg/ml), Chloramphenicol (20 μg/ml), Kanamycin (50 μg/ml), Gentamicin (30 μg/ml). For inducible plasmids, 100μM isopropyl-β-d-thiogalactopyranoside (IPTG) or 0.02%(w/v) L-arabinose were added as indicated in the figures or legends. To monitor cell growth, optical density was measured at 600nm (OD_{600}).

Gene deletions in *E. coli* MG1655 were generated by P1*vir* transduction of gene knockouts from the KEIO collection [61], followed by removing the FRT-flanked Kan cassette using pCP20, which encodes the FLP recombinase [62].

Expression plasmids were generated by amplifying gene sequences from the genomic DNA of wild-type strains using PCR with specific primers (available upon request). The amplified sequences were then inserted into the corresponding vectors (Table S1). All plasmid constructs were verified through DNA sequencing.

Motility assay

LB swim plates and swarm plates were solidified using 0.3% Fisher agar and 0.5% Eiken agar [Eiken Chemical Co., Japan] respectively. For swim plates, 5 μl of an overnight culture was inoculated in the center and plates incubated at 30°C for 8-12h. Swim ring diameter was measured to compare motility across strains. Swarm plates were supplemented with 0.5% glucose, poured and dried at room temperature (RT) for 1h inside Mystaire® MY-PCR prep station laminar flow, prior to inoculation. 10μl of an overnight culture grown in LB was inoculated in the center and plates were incubated at 30°C for 16~18h. For external

complementation with colanic acid or LPS, 100 μl extracts were added to swarm plates 1h after they were poured, and beads (3mm) (CoilRollers Plating Beads, Novagen Co.) were used to distribute them across the surface by gentle shaking.

Determination of c-di-GMP levels by RFI

This method employs a riboswitch based "dual-fluorescence reporter" system, where the expression of different colored fluorescent proteins is differentially regulated based on the presence of c-di-GMP, providing a visual readout of intracellular c-di-GMP levels. Here, a riboswitch that specifically binds to c-di-GMP, causes a conformational change in the RNA structure that impacts downstream gene expression of RFP (Red Fluorescent Protein). A divergent constitutively active promoter controls CFP (Cyan Fluorescent Protein) expression and normalizes the data for cell number. Relative fluorescence intensity (RFI) of the two readouts at 574 nm (TurboRFP) and 489 nm (AmCyan) is a measure of relative c-GMP levels. The final RFI value was normalized to the WT, with WT set to 1, which corresponds to approximately 8 pmol/mg protein based on calculations from previous work [63].

All c-di-GMP reporter strains were cultured overnight in gentamicin-containing medium at 37 °C with shaking at 200 rpm before being inoculated onto swim or swarm plates. The plates were incubated for 12 h (swim) or 20 h (swarm) and then stored at 4 °C for subsequent experiments. For swarm plate samples, cells were washed off the plates using PBS and resuspended to a final OD_{600} of 0.1. For swim plate samples, the central portion of the agar plate (diameter = 3 cm) was excised, transferred to a 50 mL tube, and washed with PBS. The tube was centrifuged at 1,000 × g for 10 minutes, the supernatant was discarded, and cells from the top of the agar were carefully collected using PBS and adjusted to a final OD_{600} of 0.1. Fluorescence spectra were measured using an RF-5301PC fluorescence spectrophotometer (Shimadzu, Kyoto, Japan). Samples were diluted with water to an OD_{600} of 0.1 before fluorescence measurement.

Imaging phase contrast view of the edge of a swarm

A phase-contrast microscope (Olympus BX53) equipped with a 40× phase-contrast PH1 objective was used to observe the swarm front. Swarm plates were prepared under the same conditions as described above and incubated at 30ºC for 4 hours prior to visualization. A micro cover glass (18 × 18 mm, VWR) was carefully placed on top of the swarm front and cell movements were captured using cellSens Imaging Software (Olympus Co.) at a rate of 10 frames per second, with a spatial resolution of 1004 × 997 pixels and a field of view measuring 120 × 120 μm^2 for up to 30s.

RNA sequencing analysis of swarms

analysis of *E. coli* swarm cells collected at 2, 4 and 20 h was performed by Marta Perez as part of another project. Swarm cells were harvested at 2, 4, and 20 h after inoculation. Cells were rinsed from the agar plates using a 2:1 mixture of RNAprotect Bacteria Reagent (Qiagen) and PBS and collected in 1.5 mL test tubes. A total volume of 1 mL was used to rinse all the cells present on each plate. Once collected, the bacterial suspension was vortexed for 5 seconds to mix thoroughly and then incubated at room temperature for 5 minutes. Cells were pelleted by centrifugation at 5000 x g for 10 minutes, and the supernatant was discarded. Total RNA was isolated from the cell samples treated with RNAprotect Bacteria Reagent using the RNeasy Mini Kit (Qiagen), following the enzymatic lysis and Proteinase K digestion protocol. A maximum of 6×10^8 cells were processed per column. To prevent DNA contamination, on-column DNA digestion was performed using the RNase-free DNase Set (Qiagen), following the manufacturer's instructions. RNA was eluted in 40 µL of RNase-free water and immediately kept cold.

RNA sequencing was outsourced to Novogene. RNA quality was assessed via visualization on agarose gel and determination of RNA concentration and RNA Integrity

Number (RIN) using a Bioanalyzer (Agilent). The RNA quantity used for sequencing was at least 0.5 μg, with a minimum concentration of 10 ng/μL. The RIN values were ≥6 with a smooth baseline. $OD_{260/280}$ and $OD_{260/230}$ ratios were 2.0 or higher. Sequencing was performed on the Illumina NovaSeq 6000 system with a sequencing depth of 6.7 million reads per sample and a read length of 150 bp (paired-end).

Isolation and sequencing of suppressors

The term "suppressors" refers to a scenario where the original mutation persists, but a second mutation restores the wild-type phenotype. To identify such revertants with regained enhanced motility in specific mutant background (*ΔdgcO*), mutant strains were inoculated onto swarm plates (0.5% Eiken agar, 0.5% glucose) and allowed to migrate for an additional 12h after a wild-type (WT) strain had fully covered a control plate. "Flares," representing regions of enhanced motility, were observed at the periphery of the motility halos. These regions were isolated and purified on LB agar. Individual colonies were further repurified, and their phenotypes were reconfirmed. Genomic DNA from these isolates was extracted and analyzed by Novogene. DNA samples used for sequencing had a minimum quantity of 1 μg and a concentration of at least 10 ng/μL. The $OD_{260/280}$ and $OD_{260/230}$ ratios were 2.0 or higher. Sequencing was conducted using the Illumina NovaSeq 6000 system and data were analyzed using the breseq program [64].

Quantitative reverse transcriptase PCR

E. coli cells grown on swarm plates (at 20h) were collected with PBS and resuspended in a final concentration of OD_{600}=1. RNA was then purified using Qiagen RNeasy Mini kit (Qiagen co.) according to the manufacturer protocol. RNA concentration was determined using NanoDrop™ One (Thermo Scientific). RNA (1 μg) from each sample was subjected to 1-step qPCR using SuperScript III One-Step (Thermo Fisher Sci.), according to the manufacturer protocol. qRT-PCR reactions were performed in triplicates and fluorescence detection was

performed using QuantStudio™ 7 Real-Time PCR (Thermo Fisher Sci.). RNA expression was normalized to the level of *gyrA*, a housekeeping gene control. The relative gene expression levels of *wcaJ* were calculated from cycle threshold (CT) values using the $2^{-\Delta C}$ method, where $\Delta C = CT(wcaJ) - CT(gyrA)$ [65].

Colanic acid extraction

E. coli cells were grown on LB swarm plates (using the same method above) for 18h and collected with PBS, at the final concentration of 1x10^10 cells/ml then heated at 100℃ for 20 min. Samples were then cooled to RT and centrifuged at 13,000 × g for 10 min. The supernatant was mixed with 3 volumes of 70% ethanol and incubated in -20℃ for 12h. After a precipitate formed at the bottom of tube, samples were centrifuged at 13,000 x g for 10 min and dried next to flame to remove the residual ethanol. Dried samples were dissolved in 100µl distilled water.

Colanic acid (CA) levels were measured by modification of the following method [66]: 50 µl of prepared extracts were then mixed with 4.5ml of H_2SO_4/H_2O (6:1 v/v) and incubated at 100℃ for 20 min. The mixture was cooled to the RT and absorbances measured at 396 nm and 427 nm. 100µl of 1M cysteine hydrochloride (cys) were then added and the absorbances measured again at 396 nm and 427 nm. Final CA concentration was measured using the following equation.

$$[OD_{396}\ cys - OD_{396}\ pre\text{-}cys] - [OD_{427}\ cys - OD_{427}\ pre\text{-}cys]$$

Extraction of LPS

LPS was extracted by hot phenol-water method as described previously with some modifications [50]. In brief, bacterial suspensions (10^{10} cells/mL) were centrifuged at 12,000×g for 10 min. The pellets were washed twice in PBS (pH = 7.2) (0.15 M) containing 0.15 mM

$CaCl_2$ and 0.5 mM $MgCl_2$. Pellets were then resuspended in 10 ml PBS and incubated at 100ºC for 20min.

To remove protein and nucleic acids, treatment with proteinase K, DNase and RNase was performed prior to extraction step. Proteinase K (50 µg/mL) (Roche, Mannheim, Germany) was added to the cell mixture and the tubes were kept at 65°C for 3h. Mixture was subsequently treated with RNase (40 µg/mL) (Roche, Mannheim, Germany) and DNase (20 µg/mL) (Roche, Mannheim, Germany) in the presence of 1 µL/mL 20% MgSO4 and incubated at 37°C overnight. An equal volume of hot (65°C) 90% phenol was added to the mixtures followed by vigorous shaking at 65°C for 15 min. Suspensions were then cooled, transferred to 1.5 mL polypropylene tubes and centrifuged at 8500×g for 15 min. Phenol phases were re-extracted by 300 µL distilled water. Sodium acetate at 0.5 M final concentration and 10 volumes of 95% ethanol were added to the extracts and samples were stored at -20°C overnight. Tubes were then centrifuged at 8000×g 4°C for 15 min and the pellets were washed twice with 95% ethanol. Pellets were resuspended in 120µl Laemmli Sample Buffer (33 mM Tris-HCl, pH 6.8, 1% SDS, 13.3% (w/v) glycerol, 0.005% bromophenol blue). Samples were then heated at 100℃ for 10 min.

Silver staining of LPS

LPS samples were boiled for 5 min prior to electrophoresis. 10 µL of each sample ($1x10^9$ cells) was separated on 15% SDS polyacrylamide gel with a 5% stacking gel at 100 mA for 2h. Silver and Coomassie blue staining of the gels was performed according to the standard protocols. The gel was washed 3x with ddH2O and transferred to an oxidizing solution (0.7 g periodic acid, 40 ml EtOH, 5 ml acetic acid, 55 ml H_2O) for 20 min on a shaking platform. The gel was again washed 3x times with water and incubated with the silver staining solution [(28 ml 0.1 N NaOH, 2 ml ammonium hydroxide (29.4%), 115 ml H_2O, 5 ml 20% silver nitrate (w/v)] for 10 min on the shaker. The gel was re-washed 3x with water and incubated with a color developer

solution (200 µl 5% citric acid, 100 µl 37% formaldehyde, 200 ml H_2O) for 10 min. Developing was stopped with 10% acetic acid. A digital camera was used to image the gels.

Biofilm assay

Cells were propagated in 96-well plates. After 20-hour incubation at 37℃, plates were washed twice with water and dried for 2 h at RT. 125µl of 0.01% Crystal violet solution (w/v) was added to each well and incubated in RT for 15 min. The plate was re-washed three times with water and then 125µl 30% Acetic acid (v/v) were added to each well. After 15 min incubation in RT, solutions in each well were transferred to a new 96 well plate. O.D. 550nm was used to measure biofilm formation, and OD_{600} for data normalization.

Contact angle measurement

Water or bacterial culture supernatant drops 10 µl in volume were placed on the outer side of the bottom part of 100 × 15-mm plastic Petri dishes (0875712; Fisher Scientific). The Petri dishes were washed with ethanol. For small angles of contact, where sideview images are not accurate, i.e. <30º, the diameter of each drop was determined by taking a close-up, top-view picture of the drop using a 10-megapixel camera (EOS R6 Mark II, Canon) with a 60-mm lens. Pictures were taken 5 min after drop deposition. The angle of contact, θ (°), between drop and surface was determined using a spherical-cap-shaped approximation for small angles ($\theta < 30°$) through θ=720·Vπ2·a3 (where V is the volume of the drop (10 μl), and a is the radius (mm) of the circle formed by the drop base) as previously described [21].

References

1. Jenal, U., A. Reinders, and C. Lori, *Cyclic di-GMP: second messenger extraordinaire.* Nature Reviews Microbiology, 2017. **15**(5): p. 271-284.
2. Povolotsky, T.L. and R. Hengge, *'Life-style' control networks in Escherichia coli: signaling by the second messenger c-di-GMP.* J Biotechnol, 2012. **160**(1-2): p. 10-6.
3. Hengge, R., *Principles of c-di-GMP signalling in bacteria.* Nature Reviews Microbiology, 2009. **7**(4): p. 263-273.
4. Hengge, R., et al., *Systematic Nomenclature for GGDEF and EAL Domain-Containing Cyclic Di-GMP Turnover Proteins of Escherichia coli.* Journal of bacteriology, 2015. **198**(1): p. 7-11.
5. Boehm, A., et al., *Second messenger-mediated adjustment of bacterial swimming velocity.* Cell, 2010. **141**(1): p. 107-16.
6. Pesavento, C., et al., *Inverse regulatory coordination of motility and curli-mediated adhesion in Escherichia coli.* Genes & development, 2008. **22**(17): p. 2434-2446.
7. Sanchez-Torres, V., H. Hu, and T.K. Wood, *GGDEF proteins YeaI, YedQ, and YfiN reduce early biofilm formation and swimming motility in Escherichia coli.* Appl Microbiol Biotechnol, 2011. **90**(2): p. 651-8.
8. Paul, K., et al., *The c-di-GMP binding protein YcgR controls flagellar motor direction and speed to affect chemotaxis by a "backstop brake" mechanism.* Mol Cell, 2010. **38**(1): p. 128-39.
9. Fang, X. and M. Gomelsky, *A post-translational, c-di-GMP-dependent mechanism regulating flagellar motility.* Mol Microbiol, 2010. **76**(5): p. 1295-305.
10. Girgis, H.S., et al., *A comprehensive genetic characterization of bacterial motility.* PLoS Genet, 2007. **3**(9): p. 1644-60.
11. Han, Q., et al., *Flagellar brake protein YcgR interacts with motor proteins MotA and FliG to regulate the flagellar rotation speed and direction.* Front Microbiol, 2023. **14**: p. 1159974.
12. Hou, Y.J., et al., *Structural insights into the mechanism of c-di-GMP-bound YcgR regulating flagellar motility in Escherichia coli.* J Biol Chem, 2020. **295**(3): p. 808-821.
13. Nieto, V., et al., *Under Elevated c-di-GMP in Escherichia coli, YcgR Alters Flagellar Motor Bias and Speed Sequentially, with Additional Negative Control of the Flagellar Regulon via the Adaptor Protein RssB.* J Bacteriol, 2019. **202**(1).
14. Valentini, M. and A. Filloux, *Multiple Roles of c-di-GMP Signaling in Bacterial Pathogenesis.* Annu Rev Microbiol, 2019. **73**: p. 387-406.
15. Limoli, D.H., C.J. Jones, and D.J. Wozniak, *Bacterial Extracellular Polysaccharides in Biofilm Formation and Function.* Microbiol Spectr, 2015. **3**(3).
16. Tuson, H.H. and D.B. Weibel, *Bacteria-surface interactions.* Soft Matter, 2013. **9**(18): p. 4368-4380.
17. Partridge, J.D. and R.M. Harshey, *Swarming: flexible roaming plans.* J Bacteriol, 2013. **195**(5): p. 909-18.

18. Kearns, D.B., *A field guide to bacterial swarming motility.* Nat Rev Microbiol, 2010. **8**(9): p. 634-44.
19. Partridge, J.D. and R.M. Harshey, *Flagellar protein FliL: A many-splendored thing.* Mol Microbiol, 2024. **122**(4): p. 447-454.
20. Chen, B.G., L. Turner, and H.C. Berg, *The wetting agent required for swarming in Salmonella enterica serovar typhimurium is not a surfactant.* J Bacteriol, 2007. **189**(23): p. 8750-3.
21. Be'er, A. and Rasika M. Harshey, *Collective Motion of Surfactant-Producing Bacteria Imparts Superdiffusivity to Their Upper Surface.* Biophysical Journal, 2011. **101**(5): p. 1017-1024.
22. Partridge, J.D. and R.M. Harshey, *More than motility: Salmonella flagella contribute to overriding friction and facilitating colony hydration during swarming.* J Bacteriol, 2013. **195**(5): p. 919-29.
23. Harshey, R.M. and T. Matsuyama, *Dimorphic transition in Escherichia coli and Salmonella typhimurium: surface-induced differentiation into hyperflagellate swarmer cells.* Proc Natl Acad Sci U S A, 1994. **91**(18): p. 8631-5.
24. Harshey, R.M., *Swarming Adventures.* , in *The lure of bacterial genetics: a tribute to JohnRoth*, J.C.K.T.H. S.M. Maloy, Editor. 2010, American Society for Microbiology: Washington, D.C. p. 163-72.
25. Toguchi, A., et al., *Genetics of swarming motility in Salmonella enterica serovar Typhimurium: critical role for lipopolysaccharide.* Journal of bacteriology, 2000. **182**(22): p. 6308-6321.
26. Ping, L., et al., *Osmotic pressure in a bacterial swarm.* Biophys J, 2014. **107**(4): p. 871-8.
27. Wang, Q., et al., *Sensing wetness: a new role for the bacterial flagellum.* Embo j, 2005. **24**(11): p. 2034-42.
28. Mariconda, S., Q. Wang, and R.M. Harshey, *A mechanical role for the chemotaxis system in swarming motility.* Mol Microbiol, 2006. **60**(6): p. 1590-602.
29. Wang, Q., et al., *Gene expression patterns during swarming in Salmonella typhimurium: genes specific to surface growth and putative new motility and pathogenicity genes.* Mol Microbiol, 2004. **52**(1): p. 169-87.
30. Junkermeier, E.H. and R. Hengge, *Local signaling enhances output specificity of bacterial c-di-GMP signaling networks.* Microlife, 2023. **4**: p. uqad026.
31. Lindenberg, S., et al., *The EAL domain protein YciR acts as a trigger enzyme in a c-di-GMP signalling cascade in E. coli biofilm control.* Embo j, 2013. **32**(14): p. 2001-14.
32. Serra, D.O. and R. Hengge, *A c-di-GMP-Based Switch Controls Local Heterogeneity of Extracellular Matrix Synthesis which Is Crucial for Integrity and Morphogenesis of Escherichia coli Macrocolony Biofilms.* Journal of Molecular Biology, 2019. **431**(23): p. 4775-4793.
33. Puri, D., X. Fang, and K.R. Allison, *Evidence of a possible multicellular life cycle in Escherichia coli.* iScience, 2023. **26**(1): p. 105795.
34. Barnhart, M.M. and M.R. Chapman, *Curli biogenesis and function.* Annu Rev Microbiol, 2006. **60**: p. 131-47.
35. Tuckerman, J.R., et al., *An oxygen-sensing diguanylate cyclase and phosphodiesterase couple for c-di-GMP control.* Biochemistry, 2009. **48**(41): p. 9764-74.

36. Tagliabue, L., et al., *The diguanylate cyclase YddV controls production of the exopolysaccharide poly-N-acetylglucosamine (PNAG) through regulation of the PNAG biosynthetic pgaABCD operon.* Microbiology (Reading), 2010. **156**(Pt 10): p. 2901-2911.
37. Zhou, H., et al., *Characterization of a natural triple-tandem c-di-GMP riboswitch and application of the riboswitch-based dual-fluorescence reporter.* Sci Rep, 2016. **6**: p. 20871.
38. Bhattacharyya, S., et al., *Efflux-linked accelerated evolution of antibiotic resistance at a population edge.* Molecular Cell, 2022. **82**(22): p. 4368-4385.e6.
39. Chen, G., et al., *Structural basis for diguanylate cyclase activation by its binding partner in Pseudomonas aeruginosa.* Elife, 2021. **10**.
40. Xu, Z., et al., *Interplay between the bacterial protein deacetylase CobB and the second messenger c-di-GMP.* Embo j, 2019. **38**(18): p. e100948.
41. Bhattacharyya, S., et al., *A heritable iron memory enables decision-making in Escherichia coli.* Proc Natl Acad Sci U S A, 2023. **120**(48): p. e2309082120.
42. Lin, C.-S., et al., *An iron detection system determines bacterial swarming initiation and biofilm formation.* Scientific Reports, 2016. **6**(1): p. 36747.
43. Beloin, C., A. Roux, and J.M. Ghigo, *Escherichia coli biofilms.* Curr Top Microbiol Immunol, 2008. **322**: p. 249-89.
44. Tamayo, R., J.T. Pratt, and A. Camilli, *Roles of cyclic diguanylate in the regulation of bacterial pathogenesis.* Annual review of microbiology, 2007. **61**: p. 131-148.
45. Cowles, K.N., et al., *Diguanylate Cyclases AdrA and STM1987 Regulate Salmonella enterica Exopolysaccharide Production during Plant Colonization in an Environment-Dependent Manner.* Appl Environ Microbiol, 2016. **82**(4): p. 1237-1248.
46. McCarthy, R.R., et al., *Cyclic-di-GMP regulates lipopolysaccharide modification and contributes to Pseudomonas aeruginosa immune evasion.* Nat Microbiol, 2017. **2**: p. 17027.
47. Serra, D.O., A.M. Richter, and R. Hengge, *Cellulose as an architectural element in spatially structured Escherichia coli biofilms.* J Bacteriol, 2013. **195**(24): p. 5540-54.
48. Wang, C., et al., *Colanic acid biosynthesis in Escherichia coli is dependent on lipopolysaccharide structure and glucose availability.* Microbiol Res, 2020. **239**: p. 126527.
49. Wang, Z., et al., *Deletion of the genes waaC, waaF, or waaG in Escherichia coli W3110 disables the flagella biosynthesis.* J Basic Microbiol, 2016. **56**(9): p. 1021-35.
50. Rezania, S., et al., *Extraction, Purification and Characterization of Lipopolysaccharide from Escherichia coli and Salmonella typhi.* Avicenna J Med Biotechnol, 2011. **3**(1): p. 3-9.
51. Tan, L. and P.S. Grewal, *Comparison of two silver staining techniques for detecting lipopolysaccharides in polyacrylamide gels.* J Clin Microbiol, 2002. **40**(11): p. 4372-4.
52. Kim, W. and M.G. Surette, *Metabolic differentiation in actively swarming Salmonella.* Mol Microbiol, 2004. **54**(3): p. 702-14.
53. Inoue, T., et al., *Genome-wide screening of genes required for swarming motility in Escherichia coli K-12.* J Bacteriol, 2007. **189**(3): p. 950-7.
54. Wang, X., J.F. Preston, 3rd, and T. Romeo, *The pgaABCD locus of Escherichia coli promotes the synthesis of a polysaccharide adhesin required for biofilm formation.* J Bacteriol, 2004.

186(9): p. 2724-34.

55. Hammar, M., et al., *Expression of two csg operons is required for production of fibronectin- and congo red-binding curli polymers in Escherichia coli K-12.* Mol Microbiol, 1995. **18**(4): p. 661-70.
56. Serra, D.O., G. Klauck, and R. Hengge, *Vertical stratification of matrix production is essential for physical integrity and architecture of macrocolony biofilms of Escherichia coli.* Environ Microbiol, 2015. **17**(12): p. 5073-88.
57. Rahman, M.M., et al., *The structure of the colony migration factor from pathogenic Proteus mirabilis. A capsular polysaccharide that facilitates swarming.* J Biol Chem, 1999. **274**(33): p. 22993-8.
58. Boles, B.R. and L.L. McCarter, *Vibrio parahaemolyticus scrABC, a novel operon affecting swarming and capsular polysaccharide regulation.* J Bacteriol, 2002. **184**(21): p. 5946-54.
59. Berg, H.C., *Swarming Motility: It Better Be Wet.* Current Biology, 2005. **15**(15): p. R599-R600.
60. Kitanishi, K., et al., *Important roles of Tyr43 at the putative heme distal side in the oxygen recognition and stability of the Fe(II)-O2 complex of YddV, a globin-coupled heme-based oxygen sensor diguanylate cyclase.* Biochemistry, 2010. **49**(49): p. 10381-93.
61. Baba, T., et al., *Construction of Escherichia coli K-12 in-frame, single-gene knockout mutants: the Keio collection.* Mol Syst Biol, 2006. **2**: p. 2006.0008.
62. Datsenko, K.A. and B.L. Wanner, *One-step inactivation of chromosomal genes in Escherichia coli K-12 using PCR products.* Proceedings of the National Academy of Sciences, 2000. **97**(12): p. 6640-6645.
63. Zhou, H., et al., *Characterization of a natural triple-tandem c-di-GMP riboswitch and application of the riboswitch-based dual-fluorescence reporter.* Scientific Reports, 2016. **6**(1): p. 20871.
64. Deatherage, D.E. and J.E. Barrick, *Identification of mutations in laboratory-evolved microbes from next-generation sequencing data using breseq.* Methods Mol Biol, 2014. **1151**: p. 165-88.
65. Livak, K.J. and T.D. Schmittgen, *Analysis of relative gene expression data using real-time quantitative PCR and the 2(-Delta Delta C(T)) Method.* Methods, 2001. **25**(4): p. 402-8.
66. Obadia, B., et al., *Influence of tyrosine-kinase Wzc activity on colanic acid production in Escherichia coli K12 cells.* J Mol Biol, 2007. **367**(1): p. 42-53.
67. Hwang, Y. and R.M. Harshey, *A Second Role for the Second Messenger Cyclic-di-GMP in E. coli: Arresting Cell Growth by Altering Metabolic Flow.* mBio, 2023. **14**(2): p. e0061923.
68. Kitagawa, M., et al., *Complete set of ORF clones of Escherichia coli ASKA library (a complete set of E. coli K-12 ORF archive): unique resources for biological research.* DNA Res, 2005. **12**(5): p. 291-9.

Main Figures

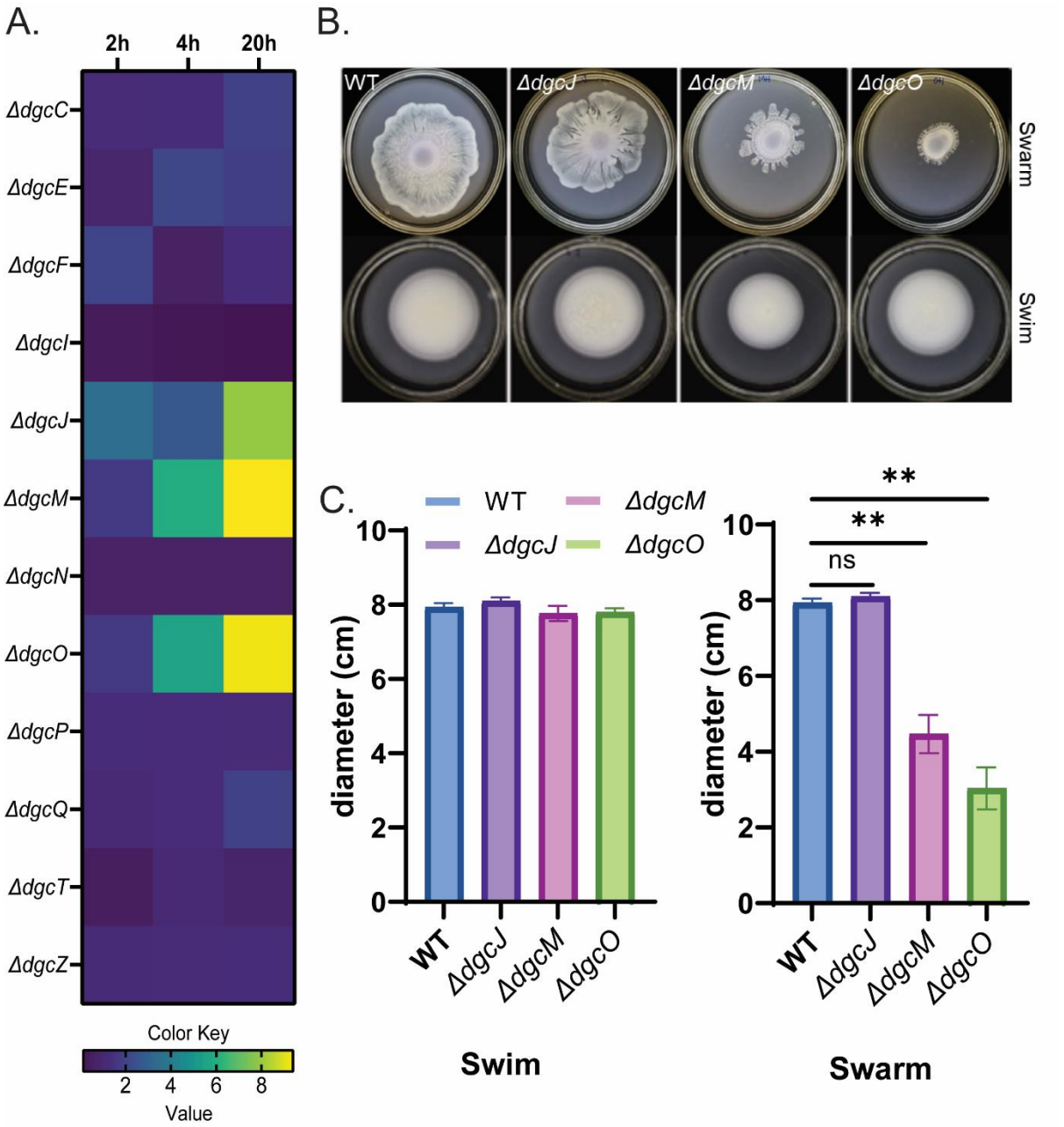

Figure 1. Identification of DGCs that contribute to swarming motility. (A) Comparison of fold changes in gene expression of WT E. coli DGCs during the time course of swarming. RNA-Seq data collected at 2, 4 and 20h during the time course of swarming were normalized to those from planktonic cultures (n=4). (B) Comparison of swimming and swarming motility of indicated DGC deletion mutants in the WT strain. Plates were incubated at 30℃ for 18h (n=3). (C) Diameters across the zones of bacterial swimming or swarming shown in B were plotted. Calculated P values are indicated: *, <0.05, **, <0.01, or ***, <0.0001. NS, not statistically significant for all four independent experiments in C.

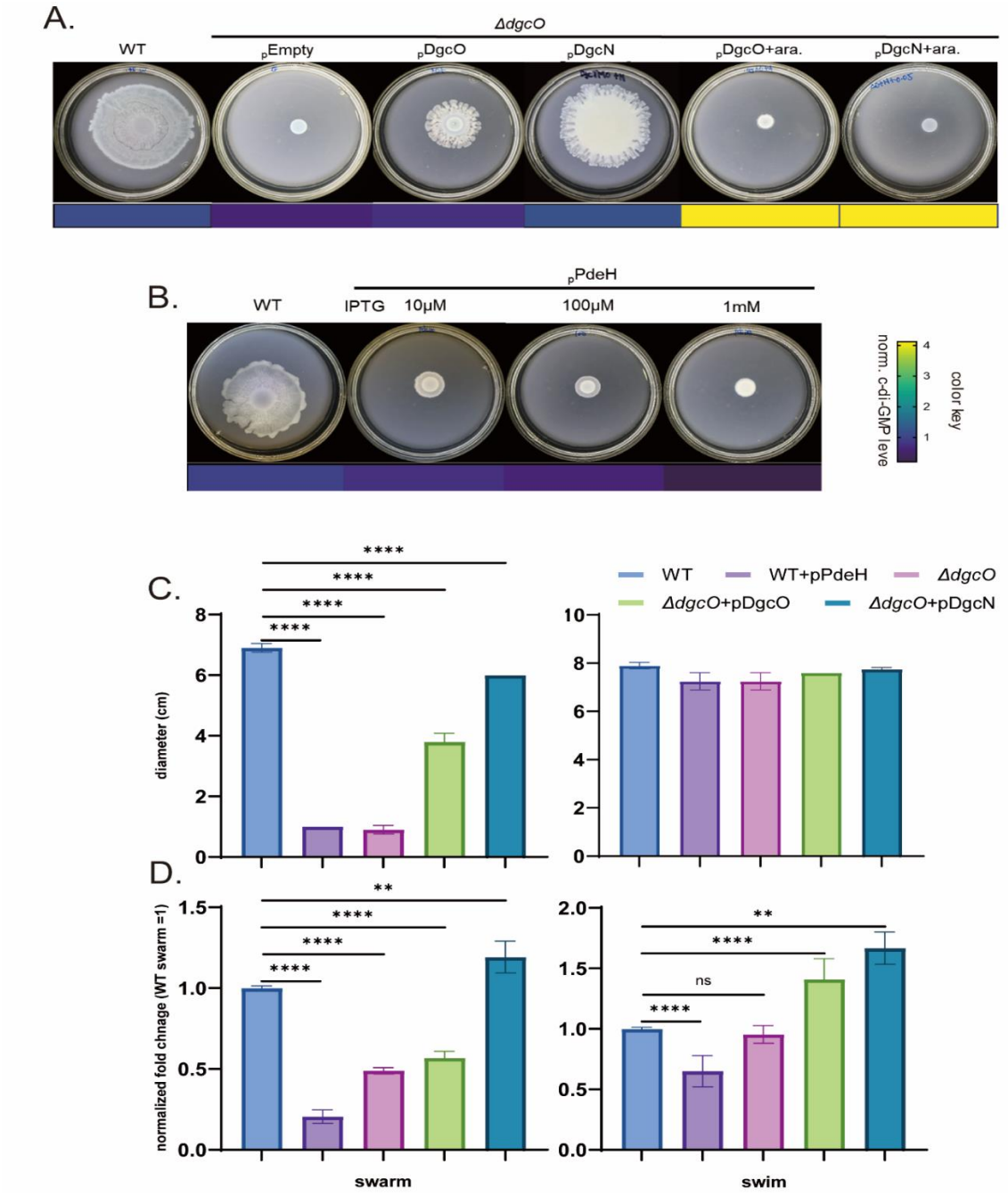

Figure 2. c-di-GMP is required for swarming. (A) Plasmids encoding *dgcO* (pDgcO), *dgcN* (pDgcN) or vector alone (pEmpty) under the control of pBAD promoter, were introduced to the *ΔdgcO* strain, and swarming compared to WT, with (+ara) or without addition of 0.05% arabinose (n=4). The color key beneath the plates corresponds to relative c-di-GMP levels measured using the riboswitch-based c-di-GMP sensor, shown in B as heatmap. (B) A plasmid encoding *pdeH* (pPdeH) was introduced into the WT strain and swarming monitored at indicated IPTG concentrations (n=2). C-di-GMP levels for all strains in this figure are found in Table1, represented here by a heat map beneath the plates. (C) Diameters of swim and swarm zones of strains indicated by a color key (n=4). (D) Cells from swim/swarm plates in C were collected and c-di-GMP levels measured using the c-di-GMP biosensor. The values were normalized to the c-di-GMP levels in WT swarm. Calculated *P* values are indicated: *, <0.05, **, <0.01, or ***, <0.0001. NS, not statistically significant. Color key as in C.

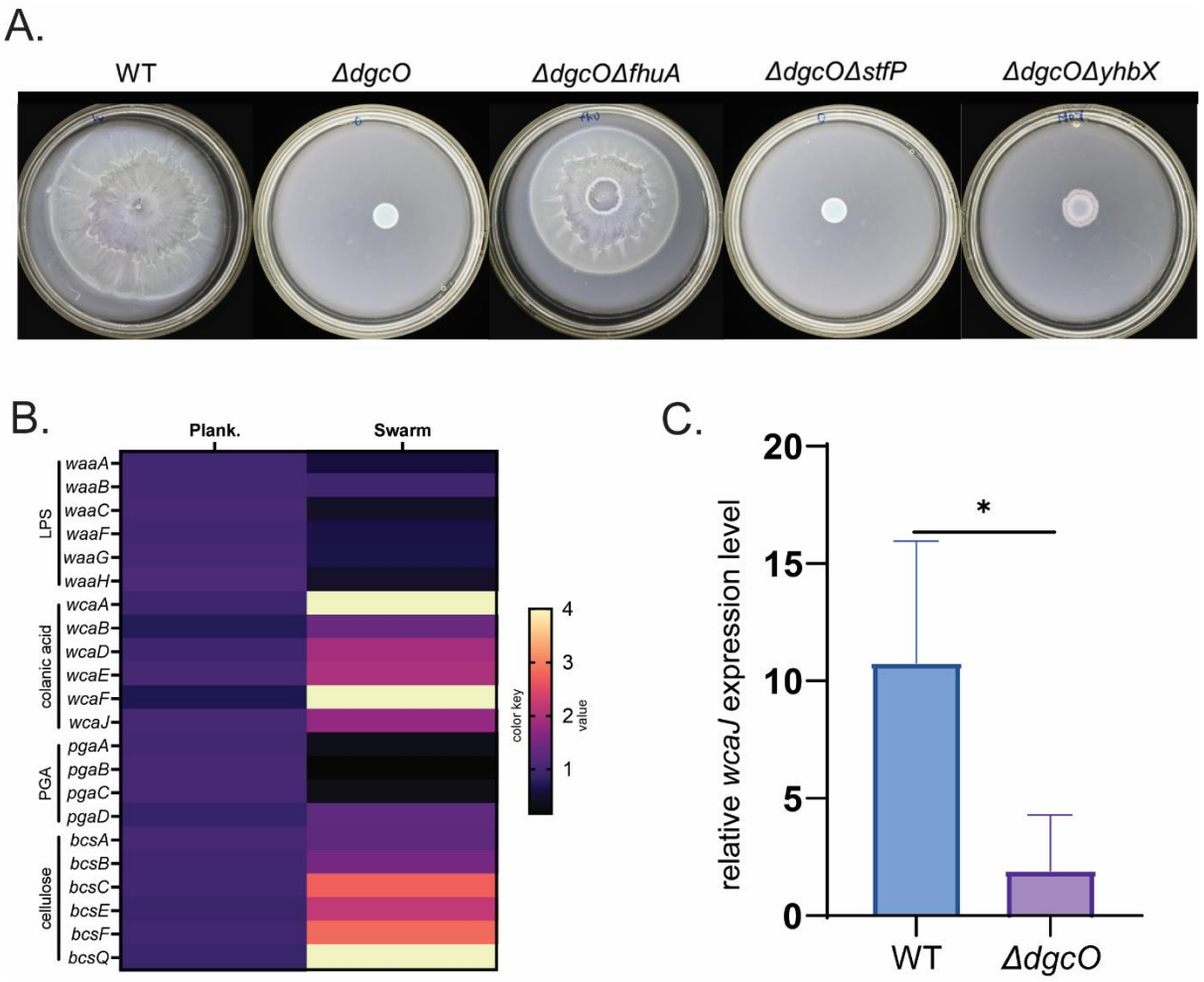

Figure 3. Suppressor analysis of *ΔdgcO.* (A) Comparison of swarming motility of WT, *ΔdgcO, ΔdgcOΔfhuA*, *ΔdgcOΔstfP, and ΔdgcOΔyhbX* strains. (B) Comparison of fold changes in gene expression of the four exopolymers of *E. coli* (LPS, colanic acid, PGA, and cellulose) during swarming. RNA-Seq data collected at 20h during the time course of swarming were normalized to those from planktonic cultures (n=4). (C) Comparison of *wcaJ* expression levels relative to *gyrA* in WT and *ΔdgcO,* using qRT-PCR from swarm cells collect at 20h (see Methods).

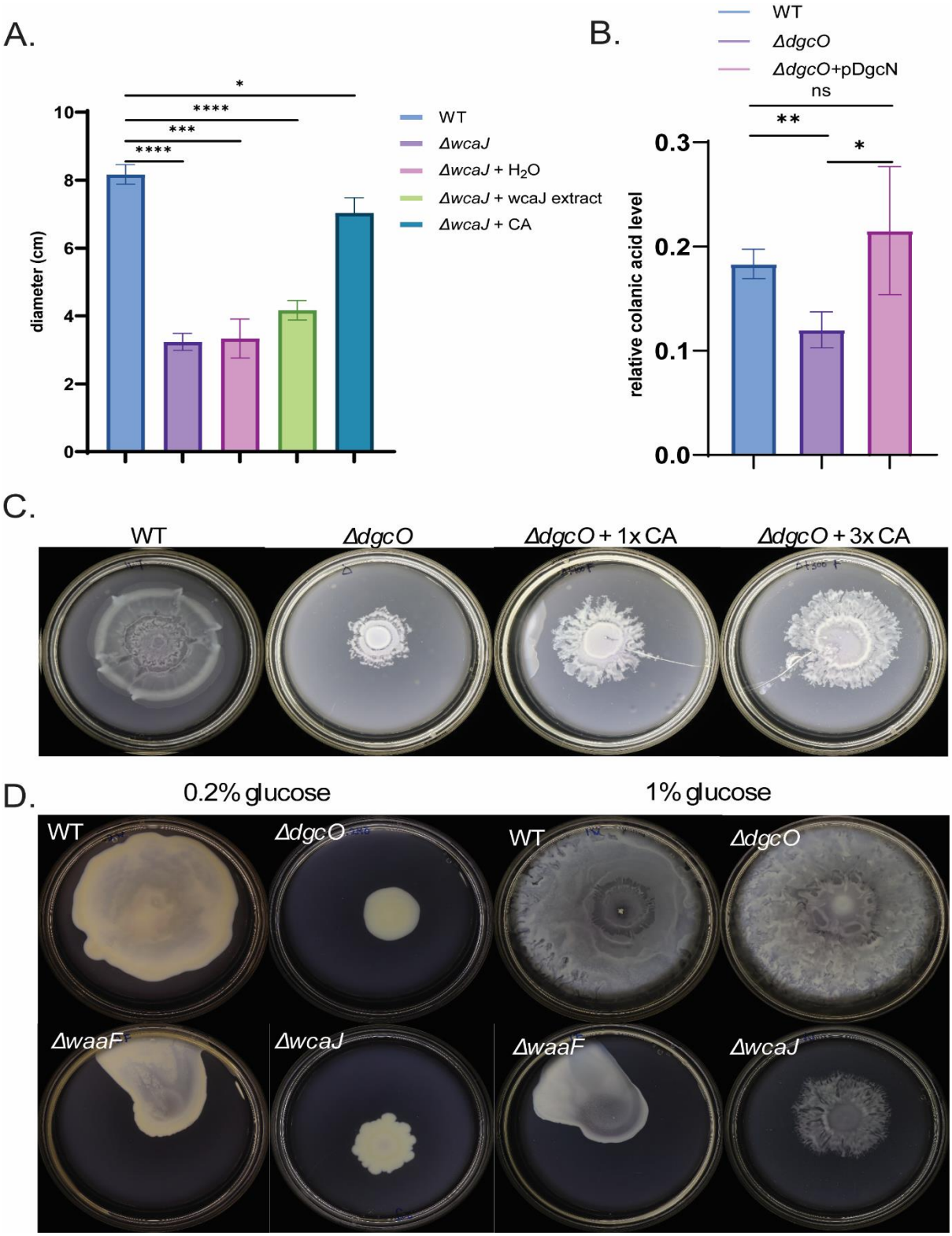

Figure 4. Colanic acid (CA) is required for swarming. (A) Swarming diameters at 20h were compared between WT, *ΔwcaJ* and *ΔwcaJ* supplemented with 100µl of either water, *ΔwcaJ* extract, or *ΔwaaF* extract (n=3). (B) Comparison of relative CA levels between WT, *ΔdgcO* and *ΔdgcO* complemented with pDgcN (n=3). CA levels were measured as described under Methods. (C) Rescue of swarming in *ΔdgcO* by addition of indicated concentrations of CA extract from *ΔwaaF*. (D) Swarming recorded at 20h on plates supplied with two different glucose concentrations (0.2% or 1%) and inoculated with indicated strains.

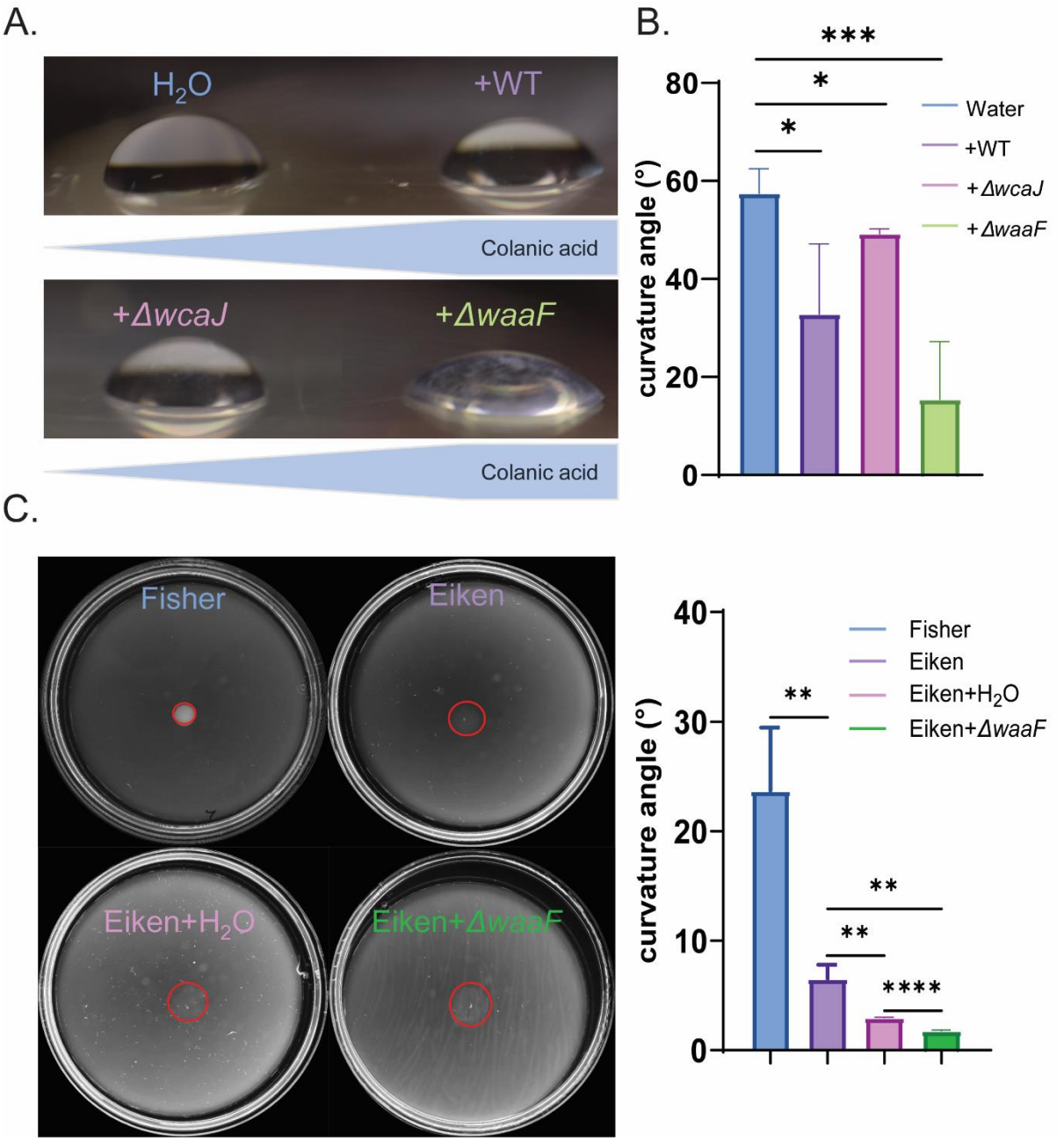

Figure 5. Colanic acid acts as a surfactant. (A) A side view of a 10-µl water drop or CA extracts in water from indicated strains, deposited on a plastic surface. Extracts with more CA are indicated in the blue ribbon below the images. The large contact angles could be measured directly from the image (see Methods). (B) A summary of measurements of contact angles from A. (C) Same as A-B, except water drops were placed directly on swarm media set with Fisher or Eiken agar (top row of plates), or water drops on Eiken agar compared with those of D*waaF* CA extract (bottom row of plates).

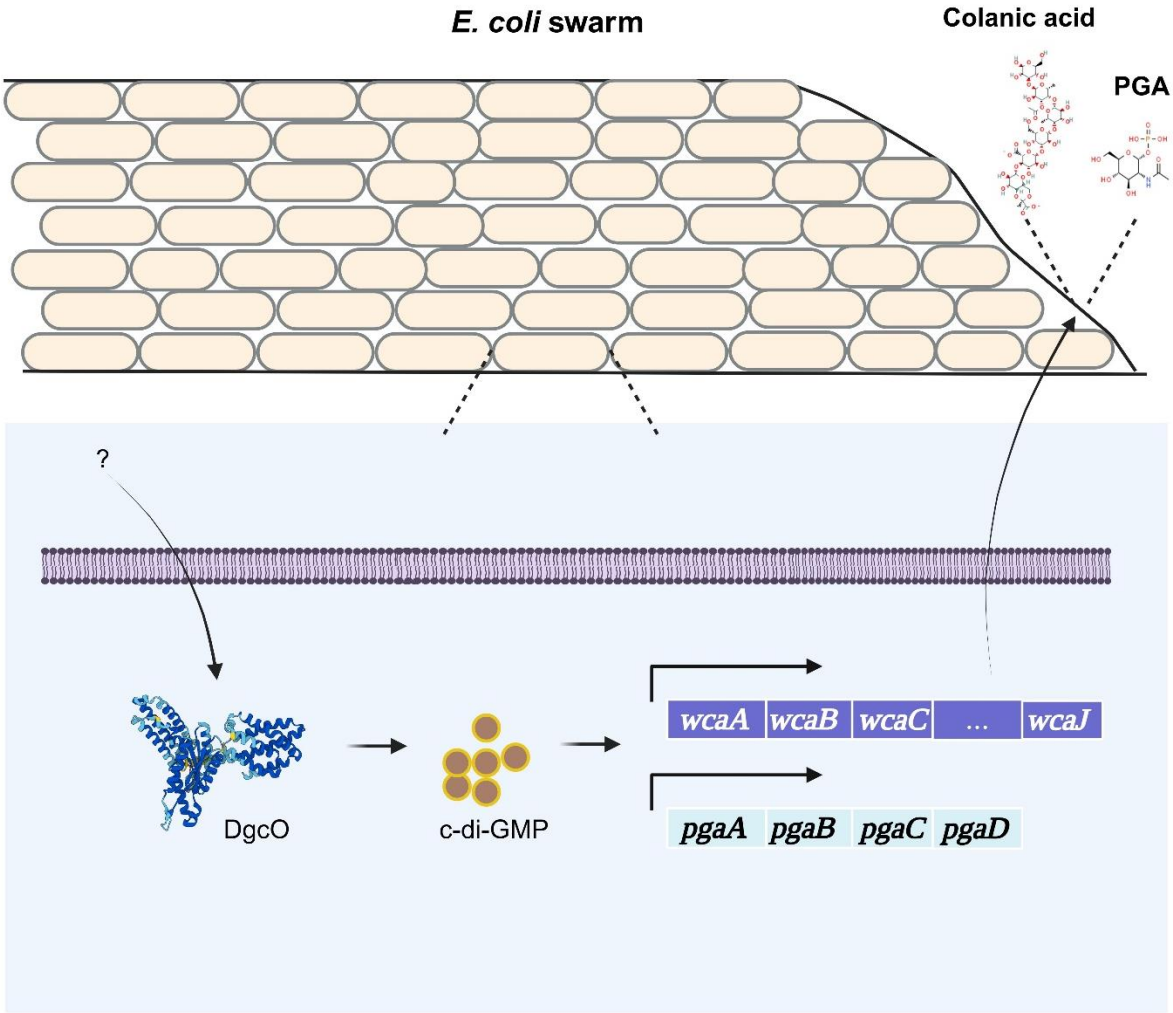

Figure 6. Summary of the role of DgcO in swarming. DgcO positively regulates swarming motility by promoting the synthesis of CA and PGA. During the swarming process, *dgcO* expression is upregulated, leading to an increase in intracellular c-di-GMP levels, which result in upregulation of CA (*wca* operon) and PGA (*pga* operon) biosynthesis pathways, both of which promote efficient swarming depending on wet/dry surface conditions.

Supplementary Figures and Tables

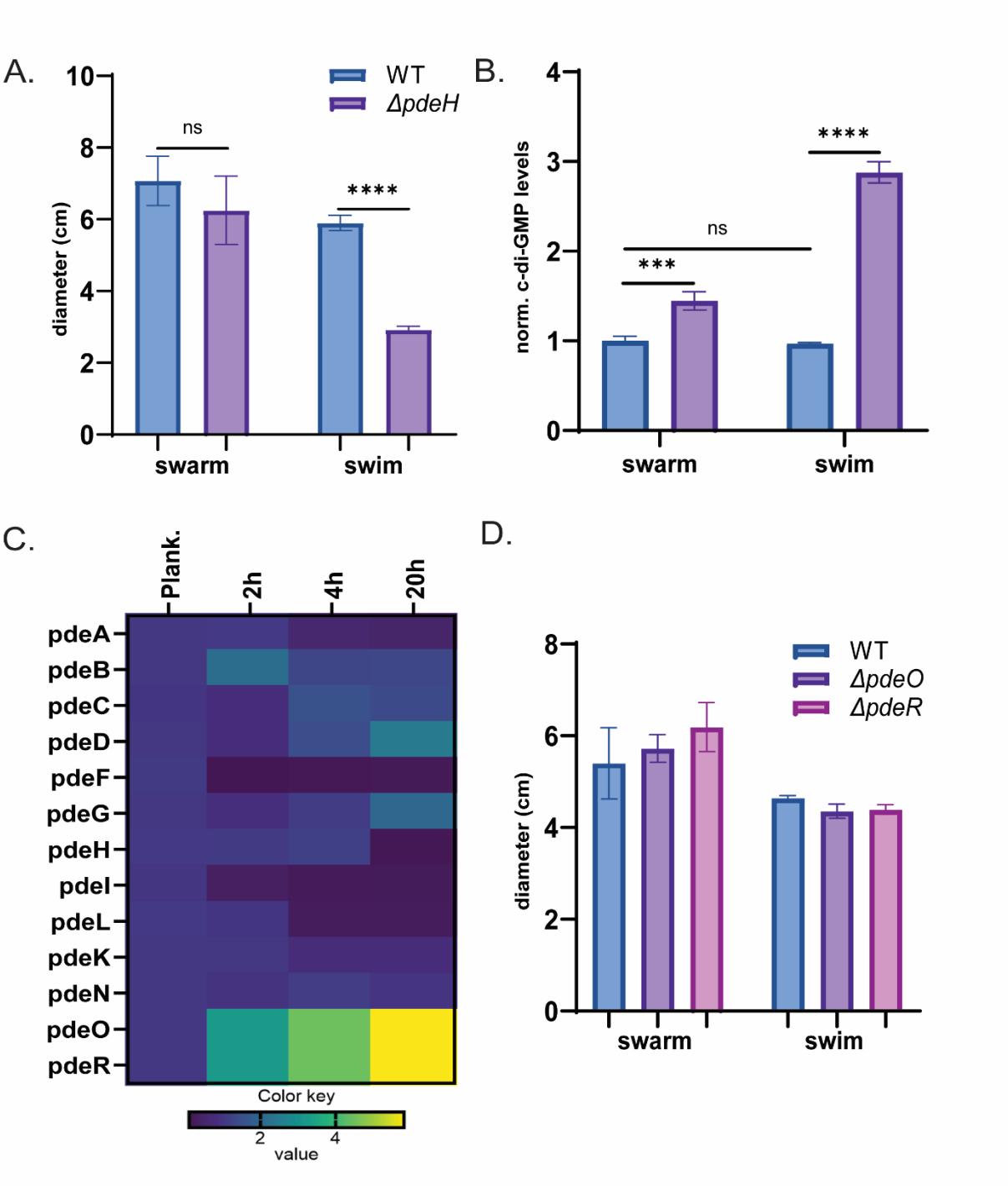

Figure S1. Differential c-di-GMP levels in swimming and swarming. (A) Comparison of motility in swim (0.3% agar) or swarm (0.5% agar) plates of WT (MG1655) and Δ*pdeH* strains. Plates were incubated at 30℃ for 18h (n=3). (B) Measurement of c-di-GMP levels using a riboswitch-based c-di-GMP sensor in cells collected from swim and swarm plates shown in A (see Methods). Color coding of strains as in A. RFP/GFP ratios were normalized to those observed in a WT swarm. (C) Comparison of fold-changes in gene expression of all the *E. coli* PDEs during the time course of swarming. RNA-Seq data collected at 2, 4 and 20 h of swarming were normalized to those from planktonic cultures (n=4). (D) Swim and swarm motility comparison of WT, Δ*pdeO* and Δ*pdeR* strains as in A.

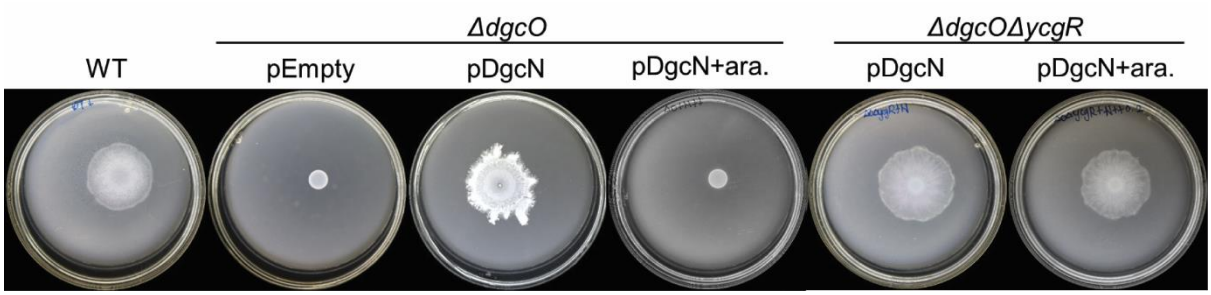

Figure S2. Swarming inhibition of pDgcN induction is through YcgR. Experimental setup as in Figure 2A except also monitored in a *ΔdgcOΔycgR* strain.

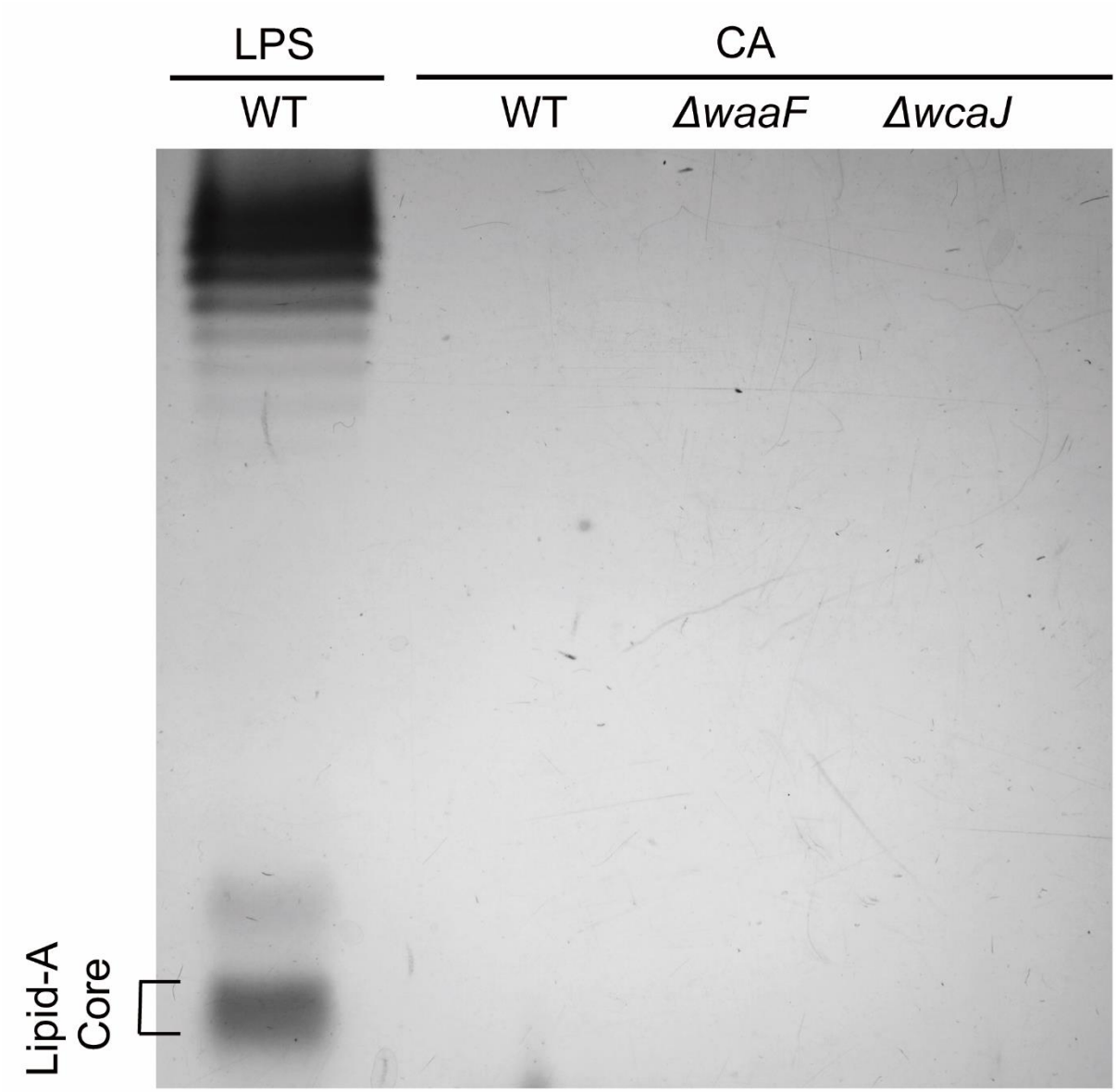

Figure S3. LPS-profiles of WT and CA extracts from mutants. LPS extract from WT and CA extracts from *ΔwaaF*, and *ΔwcaJ* strains were fractionated on SDS-PAGE gel, followed by silver staining (see Methods).

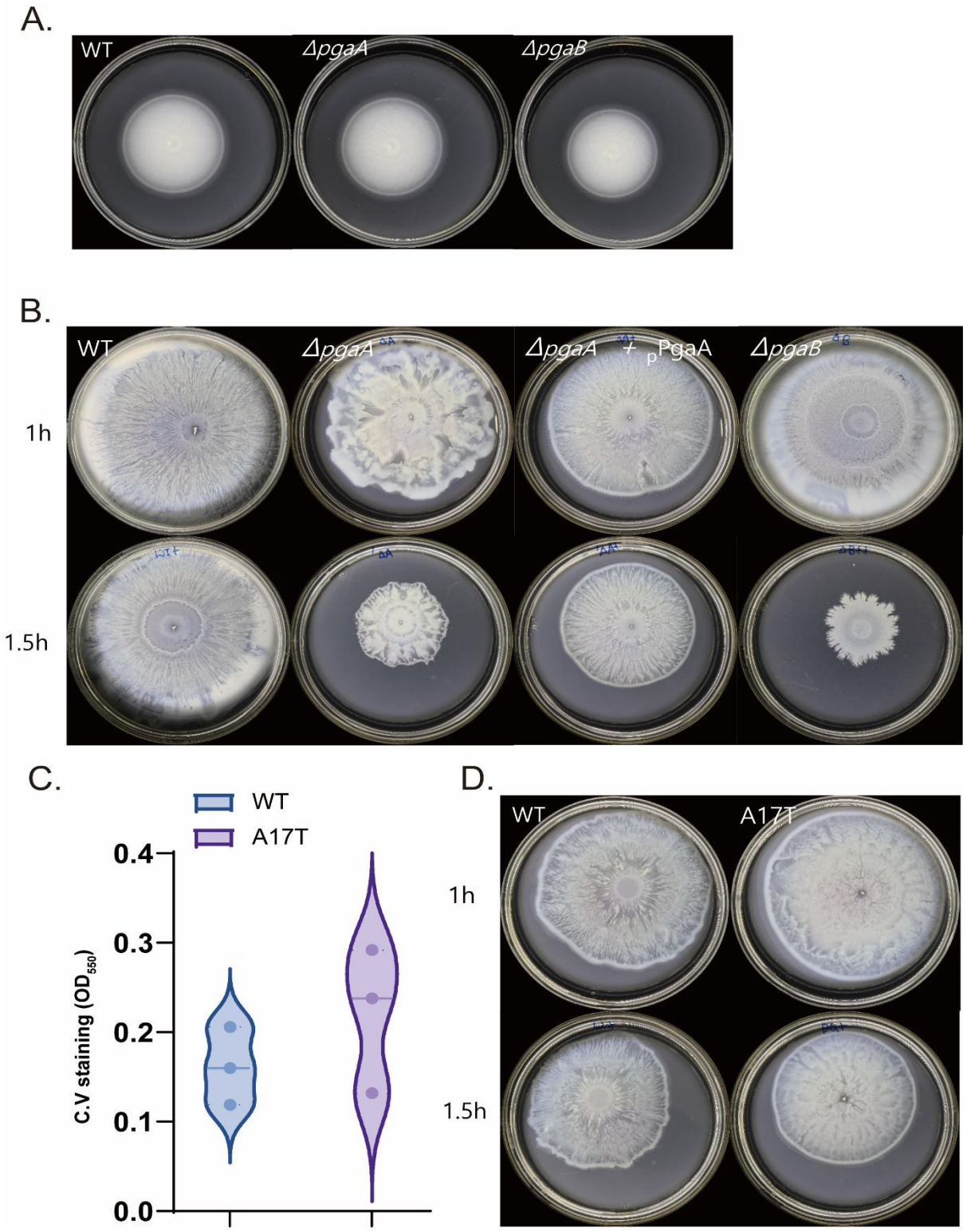

Figure S4. PGA, but not cellulose, assists swarming motility. (A-B) Comparison of swimming and swarming motility of indicated PGA deletion mutants in MG1655. Plates were incubated at 30℃ for 18h (n=3) swarm or 37℃ for 12h (n=3) swim. Swarm plates were either dried under the hood for 1h (standard condition) or 1.5h. (C) Biofilm levels measured levels at OD_{550nm} by crystal violet staining of WT and *bcsQ*(A17T). (D) Swarming recorded using strains as in C. Plates were dried for either 1 or 1.5h before cells were inoculated and incubated at 30℃ for 18h.

Movie S1. Phase contrast view of the edge of a WT swarm. Cells inoculated on swarm agar (see Methods) were viewed under phase contrast after 4h of incubation at 30ºC, a time when movement is generally first observed. The movie is in real time, at 40x magnification.

Movie S2. Phase contrast view of the edge of a Δ*dgcO* swarm. Experimental protocol was as described in Movie S1.

Movie S3 and S4. Movement at the edge WT *E. coli* swarm under different glucose concentrations. Experimental conditions as described for Movie S1, except plates were supplemented with either 0% glucose (Movie S3) or 0.5% glucose (Movie S4).

Table 1

Strain	Relative c-di-GMP level to WT	Condition
WT(MG1655)	1±0.015	Swim
Δ*pdeH*	3±0.5	Swim
ΔdgcO	0.875±0.02	Swim
WT+pPdeH (1mM IPTG)	0.75±0.04	Swim
ΔdgcO + pDgcO (0% ara)	1.28±0.37	Swim
ΔdgcO + pDgcN (0% ara)	1.5±0.098	Swim
ΔdgcO + pDgcN+ (0.05% ara.)	5±0.56	Swim
WT(MG1655)	1±0.015	Swarm
Δ*pdeH*	1.25±0.031	Swarm
ΔdgcM	1±0.0175	Swarm
ΔdgcO	0.625±0.0738	Swarm
ΔdgcOΔfhuA	0.75±0.0.019	Swarm
WT+pPdeH (10μM IPTG)	0.875±0.0.029	Swarm
WT+pPdeH (100μM IPTG)	0.75±0.0.019	Swarm
WT+pPdeH (1mM IPTG)	0.625±0.129	Swarm
ΔdgcO + pDgcO (0% ara)	0.75±0.234	Swarm
ΔdgcO + pDgcN (0% ara)	1.25±0.066	Swarm
ΔdgcO + pDgcO (0.05% ara)	3.125±0.75	Swarm
ΔdgcO + pDgcN+ (0.05% ara.)	5.25±0.813	Swarm

*WT=1 is roughly equivalent to 8pmol/mg protein based on the calculation from [37]

Table 2

Suppressor strain	Mutant genes	Mutations	Gene function
JH1105	*yhbX*	D105N (GAC->AAC)	putative hydrolase
	fhuA	deletion Δ1092-2244	ferrichrome porin
	stfP	deletion Δ290-309	cryptic prophage
JH1106	*yhbX*	D105N (GAC->AAC)	putative hydrolase
	fhuA	deletion Δ1092-2244	ferrichrome porin
JH1107	*yhbX*	D105N (GAC->AAC)	putative hydrolase
	fhuA	deletion Δ1670-2244	ferrichrome porin
	stfP	deletion Δ290-309	cryptic prophage
JH1108	*yhbX*	D105N (GAC->AAC)	putative hydrolase
	fhuA	deletion Δ1390-2244	ferrichrome porin
	stfP	deletion Δ290-309	cryptic prophage
JH1109	*yhbX*	D105N (GAC->AAC)	putative hydrolase
	fhuA	deletion Δ1092-2244	ferrichrome porin
JH1110	*yhbX*	D105N (GAC->AAC)	putative hydrolase
	fhuA	deletion Δ1092-2244	ferrichrome porin
JH1111	*yhbX*	D105N (GAC->AAC)	putative hydrolase
	stfP	deletion Δ290-309	cryptic prophage
JH1112	*yhbX*	D105N (GAC->AAC)	putative hydrolase
	fliT	deletion Δ344-360	flhDC repressor
	stfP	deletion Δ290-309	cryptic prophage
JH1113	*stfP*	deletion Δ290-309	cryptic prophage
	fhuA	deletion Δ1092-2244	ferrichrome porin
JH1114	*yhbX*	D105N (GAC->AAC)	putative hydrolase
	ptsG	deletion Δ355-1334	glucose phosphotransferase system
	stfp	deletion Δ290-309	cryptic prophage

Table S1

Strains	**Genotype or Description**	**Reference**
MG1655	K12 wild-type (WT) strain: F^-, λ^-, rph-1	Laboratory Collection
JH702	MG1655 Δ*dgcM*	This work
JH703	MG1655 Δ*dgcO*	This work
JH1011	MG1655 Δ*dgcO* + pBAD30_empty	This work
JH1012	MG1655 Δ*dgcO* + pBAD30_DgcO	This work
JH1013	MG1655 Δ*dgcO* + pBAD30_YfIN	This work
JH706	MG1655 Δ*waaF*	This work
JH707	MG1655 Δ*wcaJ*	This work
JH711	MG1655 + ASKA_pdeH	This work
JH1422	MG1655 Δ*dgcM* + pBAD30_empty	This work
JH1423	MG1655 Δ*dgcM* + pBAD30_DgcM	This work
JH1408	MG1655 + cdiGsens	This work
JH1409	MG1655 *ΔdgcM*+ cdiGsens	This work
JH1410	MG1655 *ΔdgcO*+ cdiGsens	This work
JH1418	MG1655 *ΔpdeH*+ cdiGsens	This work
JH1105-1114	MG1655 *ΔdgcO* suppressors	This work
JH1419	MG1655 ASKA_PdeH+cdiG sens	This work
JH1201	MG1655 Δ*dgcO*Δ*fhuA*	This work
JH1202	MG1655 Δ*dgcO*Δ*stfP*	This work
JH1203	MG1655 Δ*dgcO*Δ*yhbX*	This work
JH1204	MG1655 Δ*dgcO*Δ*fhuA*+cdiG sens	This work
Plasmids	Expressed Proteins	
pKD4	Kanamycin resistance gene template	[62]
pKD46	λ Red Recombinase	[62]
pCP20	FLP recombinase	[62]
pTrc99a	Cloning vector, $_P$Trc; Amp^R	[67]
pBAD30	Cloning vector; $_P$BAD; Amp^R	[67]

pBAD33	Cloning vector; $_{P}$BAD; Cm^{R}	[67]
pBAD30_YfiN	pBAD::YfiN	[67]
pBAD30_DgcO	pBAD:;DgcO	This study
pBAD30_DgcM	pBAD:;DgcM	This study
ASKA_PdeH	pca24N::PdeH	[68]
cdiG sens	pRP0122-P*be-amcyan_Bc4_turborfp*	[37]